



Inhibition of trehalose breakdown increases new carbon partitioning into cellulosic biomass in *Nicotiana tabacum*

Marcel Best^a, Kaitlyn Koenig^b, Kelly McDonald^c, Michael Schueller^d, Alistair Rogers^{e,f}, Richard A. Ferrieri^{d,*}

^a Fachbereich Chemie, Johannes Gutenberg Universität, 55099 Mainz, Germany

^b Quinnipiac University, Hamden, CT 06518-1908, USA

^c Marist College, Poughkeepsie, NY 12601, USA

^d Medical Department, Brookhaven National Laboratory, Upton, NY 11973, USA

^e Environmental Sciences Department, Brookhaven National Laboratory, Upton, NY 11973, USA

^f Department of Crop Sciences, University of Illinois at Urbana Champaign, IL 61801, USA

ARTICLE INFO

Article history:

Received 28 October 2010

Received in revised form 11 January 2011

Accepted 19 January 2011

Available online 25 January 2011

Keywords:

[¹³C]Cellulose

[¹³C]Hemicellulose

Metabolism

Trehalose

Trehalase

Validamycin

ABSTRACT

Validamycin A was used to inhibit in vivo trehalase activity in tobacco enabling the study of subsequent changes in new C partitioning into cellulosic biomass and lignin precursors. After 12-h exposure to treatment, plants were pulse labeled using radioactive ¹³CO₂, and the partitioning of isotope was traced into [¹³C]cellulose and [¹³C]hemicellulose, as well as into [¹³C]phenylalanine, the precursor for lignin. Over this time course of treatment, new carbon partitioning into hemicellulose and cellulose was increased, while new carbon partitioning into phenylalanine was decreased. This trend was accompanied by a decrease in phenylalanine ammonia-lyase activity. After 4 d of exposure to validamycin A, we also measured leaf protein content and key C and N metabolite pools. Extended treatment increased foliar cellulose and starch content, decreased sucrose, and total amino acid and nitrate content, and had no effect on total protein.

© 2011 Elsevier Ltd. All rights reserved.

1. Introduction

Higher plants fix atmospheric carbon dioxide producing sucrose, a mobile disaccharide that is distributed and used as a principal source of energy and carbon by the plant during growth and development. Trehalose, also a disaccharide, is the principal storage carbohydrate of bacteria, yeast cells, fungal spores, and certain invertebrates. Unlike sucrose, which consists of glucose and fructose units bound in an α,β -1,2 configuration, trehalose consists of two glucose units bound in an α,α -1,1 configuration. Sucrose, the more soluble of the two disaccharides, is better suited as a transport sugar within plants.¹ At sites where there is rapid growth, sucrose can be cleaved by invertase into glucose and fructose and used for energy production. Alternatively, sucrose synthase can cleave sucrose into uridine diphosphate glucose (UDP-glucose) and fructose, preserving the energy status of the cell while at the same time providing carbon skeletons for cell-wall polysaccharide synthesis. Cellulose, one of the primary cell-wall polysaccharides, relies on a steady supply of UDP-glucose for its synthesis.²

Higher plants possess genes that encode the enzymes trehalose-6-phosphate synthase (TPS) and trehalose-6-phosphate phosphatase (TPP) that are associated with trehalose biosynthesis.³ Furthermore, trehalase, the key enzyme responsible for the hydrolysis of trehalose during degradation, is present in all organs of higher plants, with highest activities found in the flowers.³ Even so, trehalose has been somewhat of an obscure curiosity in plants owing to the fact that it has only been observed in substantial concentrations in the resurrection plants, *Selaginella lepidophylla* and *Myrothamnus flabellifolia*.⁴ This sugar is thought to accumulate in the cells of these plants enabling them to adapt to dehydration, salinity, freezing, and heat stress.⁵ Typically, trehalose is almost undetectable in higher plants.^{1,6,7} Even so, recent literature suggests that trehalose may play a pivotal role in cellular signaling, in coordinating metabolic partitioning and as a source-sink for the allocation of carbon resources during growth and development.^{8,9} For example, up-regulation of genes associated with trehalose biosynthesis has been observed during the maturation phase of plant embryo development. This action may have relevance to cell expansion during differentiation, to increased activity of the sucrose synthase enzyme, and to altered cell-wall structure.¹⁰ Furthermore, in yeast TPS and TPP are known to form a multimeric enzymatic complex comprised of polypeptide chains that may play important regulatory roles.¹¹ Using the *tps1Δ* mutant in yeast, it was demonstrated that it was unable to grow on glucose enhanced media, giving strong evidence to suggest that the TPS1

* Corresponding author. Tel.: +1 631 344 4947; fax: +1 631 344 7350.

E-mail address: rferrieri@bnl.gov (R.A. Ferrieri).

peptide subunit may regulate cellular glucose influx.¹² The same may be true of plants. Also, there is a strong correlation between the inhibition of hexokinases in *Saccharomyces cerevisiae* by trehalose-6-phosphate (T6P), and the regulation of sugar partitioning into glycolysis, providing additional evidence to suggest that a strong tie exists between trehalose accumulation and cellular glucose utilization.^{13,14}

Based on previous work demonstrating an association between trehalose biosynthesis and altered cell-wall composition in plant embryos,⁸ and on the direct association between trehalase activity and trehalose accumulation in mature plants,¹⁵ we hypothesized that inhibition of trehalose degradation in mature plants would increase metabolic partitioning of new carbon into cell-wall polysaccharides, most notably cellulose and hemicellulose, at the expense of lignin biosynthesis.

Specifically, we used the potent trehalase inhibitor, validamycin A, to investigate the association between trehalose degradation and glucose utilization for cell-wall polysaccharide biosynthesis. Our general approach made use of the radioactive isotope ¹¹C ($t_{1/2}$ 20.4 m) that was introduced into the foliar tissue of intact plants via ¹¹CO₂ fixation,¹⁶ and we monitored the incorporation of the tracer into cell-wall [¹¹C]cellulose and [¹¹C]hemicellulose, as well as incorporation into [¹¹C]phenylalanine, the principal substrate of the phenylpropanoid pathway and lignin biosynthesis. This approach enabled us to measure the turnover of new carbon into cellulosic biomass over timelines that were far too short to allow detection of changes in composition.

2. Materials and methods

2.1. Plant materials

Tobacco plants (*Nicotiana tabacum* L. cv Samsun) were grown from seeds in commercial potting mix with a slow-release fertilizer (Osmocote) under metal-halide lamps at 24 °C with a 16/8 h at 350 μmol m⁻² s⁻¹ photoperiod. At 3 weeks into their growth cycle, the plants were removed from their growth pots and transferred to an aerated hydroponic station. Nutrients status of the hydroponics was maintained using a modified Hoagland's solution (2.4 mM CaNO₃, 3.2 mM KNO₃, 0.75 mM KH₂PO₄, 1.1 mM MgSO₄, 7.1 μM MnSO₄, 3.4 μM ZnSO₄, 0.6 μM CuSO₄, 80 μM H₃BO₃, 1 μM Na₂MoO₄ and 161.8 μM FeNa-EDTA) that was changed on a 5-d cycle. Plants were used for experiments when they had seven fully expanded leaves. Tracer studies targeted leaf-3, counting down from the top where leaf-1 was the first fully expanded leaf. Biomass measurements targeted leaf-2 and leaf-3. The same growth conditions were maintained during the application of the validamycin A treatment and labeling of recent photosynthate with ¹¹CO₂.

2.2. Treatment

Plants were treated using a solution of validamycin A that was added to the Hoagland's hydroponics solution to bring the treatment concentration to 150 μM (K_i , 10 nM). In one subset of plants, the effect of treatment after 12 h was measured relative to changes in new carbon partitioning (as ¹¹C) into cellulosic biomass of leaf-3, soluble sugars, and phenylalanine. In a second subset of plants, the effect of continued treatment over 4 d was assessed by testing for changes in foliar (leaf-2 + leaf-3) cellulose content, starch/sugar content, nitrate content, total amino acids, and soluble protein content. During the time of treatment, plants were maintained under the same photoperiod (16/8 h at 350 μmol m⁻² s⁻¹), and fresh nutrient was introduced after 3 d. Control studies were identical to those described above with the exception that no antibiotic was added to the nutrient solution.

2.3. Radiotracer production and administration

¹¹CO₂ was produced via the ¹⁴N(p,α)¹¹C nuclear transformation from 20 mL volume high-purity nitrogen gas target (500 mL @ STP) using 18 MeV protons from the TR-19 (Ebco Industries Ltd, Richmond, BC, Canada) cyclotron at Brookhaven National Laboratory, and captured on a molecular sieve (4 Å). The ¹¹CO₂ that was trapped on the molecular sieve was desorbed and quickly released into an air stream at 400 mL min⁻¹ as a discrete pulse for labeling a leaf in a 5 × 10 cm lighted (920 μmol m⁻² s⁻¹) cell.¹⁶ The extent of ¹¹C-fixation was correlated to leaf-level photosynthetic activity as measured by infrared gas exchange (Li-Cor Biosciences, Lincoln, NE USA; model 6162).

2.4. Analysis of radioactive cellulosic biomass

Forty-five minutes after the tracer was administered, the study leaf (leaf-3) was excised at the petiole. The 5 × 10 cm area exposed to the tracer was then cut away from the remaining leaf tissue, weighed, and then flash frozen in liquid nitrogen. Using a mortar and pestle, the tissue was powdered in liquid nitrogen, and extracted using standard procedures.^{17–20} In the first step the tissue was refluxed in 6 mL of aq MeOH (50% v/v) for 10 min at 90 °C. The extract was separated by pipette, and the remaining tissue was washed twice using 6 mL of deionized water. The washings were combined with the aqueous alcohol fraction prior to counting the ¹¹C. This fraction removed small soluble compounds including radiolabeled monosaccharides and disaccharides and amino acids that were subjected to separate radio-HPLC analyses discussed below. The remaining tissue (considered cell-wall components) was subjected to an extraction using 6 mL of dilute 1 N NaOH for 10 min at 95 °C. This step separated callose (1,3-β-glucans), as well as pectins (branched chain 1,4-β-glucans) from the remaining cell-wall polymers. The extract was again separated by pipette, and the remaining tissue washed twice using 6 mL of deionized water. The washings were combined with the base portion prior to counting the ¹¹C. The remaining tissue was then subjected to acid digestion using a 3:1 mixture of dilute 1 N nitric acid: acetic acid for 30 min at 100 °C enabling hemicellulose to be solubilized, leaving behind cellulose as the undigested portion. The contents were cooled to ambient temperature and filtered onto 2-cm disks of pre-weighed glass microfiber filters (GF/A: 2.5 cm diameter; Whatman, Maidstone, UK). The collected tissue was washed 3-times during this filtration step using deionized water. Samples were immediately counted using a static NaI gamma radiation detector, decay-corrected back to a common zero time and fraction-corrected to allow correlation to total ¹¹C-activity fixed within the tissue. Once counted, filtered samples were dried under a heat lamp and re-weighed to determine the amount of cellulosic biomass.

We verified that the indigestible acid portion was cellulose by re-subjecting this material to a stronger digestion using the phenol-sulfuric acid assay.²¹ This method involved refluxing the material in a 1:10 solution of phenol (5%) and concentrated sulfuric acid at 100 °C until all of the solid material was digested. Aliquots of the neutralized extract were then analyzed by HPLC for glucose levels that correlated back to the mass of cellulose digested.

2.5. Analysis of radioactive soluble sugars

A 50 μL volume of the MeOH-H₂O extract was injected onto a reversed-phase analytical HPLC column (Phenomenex, Torrance, CA, USA: Luna™ NH₂, 5 μm particle size, 250 × 4.6 mm i.d.). At injection, the mobile phase (1.5 mL m⁻¹) was sustained at 80% acetonitrile–20% H₂O. The mass levels of the soluble sugars were measured using a refractive index (RI) detector (Sonntek Inc., Upper

Saddle River, NJ, USA). The outlet of the RI detector was connected in series to a NaI gamma radiation detector (Ortec Inc, Oak Ridge TN, USA) that enabled direct measurement of the amount of radioactivity associated with each substrate eluting the column. Analog outputs from both the mass and radiation detectors were fed to a chromatography data acquisition station (SRI Instruments, Torrance, CA, USA) where integrated peak areas were measured from both inputs.

Sugars were identified by their elution times and correlated to those of authentic standards. Samples were also corrected for analytical dilutions. Changes in radioactive substrate levels were normalized to a standard amount of ^{11}C tracer that was administered to a particular leaf. To account for the 20.4-min half-life, all radioactivity data was corrected for radioactive decay by reference to a common time point in the experiment.

2.6. Analysis of radioactive phenylalanine

A second aliquot of the alcoholic extract was mixed with an equal volume of *o*-phthalaldehyde amino acid derivatizing reagent (OPA) containing 0.1% (v/v) mercaptoethanol and 0.1% (v/v) sodium hypochlorite (Sigma Life Science, St. Louis, MI, USA), and samples analyzed by reversed phase radio-HPLC (Phenomenex, Torrance, CA, USA: Ultramex™ C₁₈, 10 μm particle size, 250 × 4.6 mm i.d.) using procedures previously described by us in detail.²² Our interest here was to determine whether validamycin A treatment impacted new carbon (as ^{11}C) partitioning into phenylalanine as it is the principal substrate of the phenylpropanoid pathway that leads to cell-wall lignin. We applied the same treatment to radioactivity data as described above.

2.7. Analysis of cinnamic acid

Phenylalanine ammonia-lyase (PAL) catalyzes the formation of *trans*-cinnamic acid from phenylalanine in the first step of the phenylpropanoid pathway. PAL activity was inferred by the amount of endogenous cinnamic acid found in treated tissues. In parallel studies to that described above, leaf-3 was excised at 12 h after treatment and dried for 24 h in an oven at 70 °C. After weighing to obtain a dry mass, the tissue was extracted in tetrahydrofuran (Sigma Life Science, St. Louis, MI, USA) for 3 h at 25 °C according to a literature procedure.²³ Gas chromatography analysis was performed on aliquots of tissue extract using a non-polar fused-silica column (30 × 0.53 mm i.d.) coated with methyl silicone gum (HP-1: Hewlett–Packard Co., Rockville, MD, USA) at a film thickness of 2.65 μm. The gas chromatograph (Hewlett–Packard 5890 Series II) was equipped with a flame ionization detector operated at a temperature of 300 °C. The other instrument conditions were as follows: injector temperature, 230 °C; carrier gas, helium; carrier gas inlet pressure, 100 kPa; oven temperature, 50–250 °C at 10 °C min⁻¹. Analyses were performed using the splitless injection mode. Data was acquired using a Vision IV chromatography station (Scientific Systems, Inc., State College, PA, USA). *trans*-Cinnamic acid was identified based on its elution time matched against that from an authentic sample. Peaks were integrated and correlated to a mass amount using a calibrated detector mass–response curve.

2.8. Analysis of leaf-level carbohydrates and total nitrogen

Frozen leaf material was ground and aliquoted cryogenically using a cryo-bath and ball mill equipped with a cryo-block (2600 Cryo-Station, 2650 Cryo-Block and 2000 Geno Grinder, SPEX SamplePrep, Metuchen, NJ). Glucose, fructose, sucrose, and total free amino acids were extracted from 20 mg of the frozen powdered leaf material with sequential incubations in EtOH. Starch was extracted from the pellet resulting from the EtOH extraction and con-

verted to glucose by incubation with *exo*- and *endo*-amylases.²⁴ The glucose resulting from starch degradation and the glucose, fructose and sucrose in the ethanolic extract were assayed using a continuous enzymatic substrate assay. The protein content in the pellet was determined using the Pierce Protein Determination Kit (Pierce, Rockford, IL, USA), and total amino acid content in the EtOH extract was determined using a fluorogenic-based microplate assay.²⁵

3. Results

While validamycin A has been shown to selectively inhibit trehalase in *Arabidopsis*,^{3,15,26} we wanted to confirm its action in tobacco. We compared trehalose levels in control plants ($N = 3$) treated with 100 nM trehalose (Sigma Life Science, St. Louis, MI, USA) in Hoagland's solution with study plants ($N = 3$) treated with a combination of 100 nM trehalose and 150 μM of validamycin A in Hoagland's solution (Fig. 1). Because trehalose is such a minor sugar in higher plants, we decided to add an additional source of the sugar as a way to better observe effects of the antibiotic on enzyme inhibition. After a 12-h exposure to the combination of trehalose and validamycin A, we analyzed the MeOH–H₂O extract for levels of trehalose using our soluble sugar analysis HPLC method. The system was calibrated against an authentic α,α -trehalose standard. We found that trehalose levels in leaf-3 were 3.22 ± 1.36 times higher ($P = 0.013$) in validamycin A-treated plants than in non-treated plants.

A 12-h exposure to validamycin A resulted in a significant increase in the partitioning of ^{11}C into the acid-soluble fraction, from $11.0 \pm 1.5\%$ ($N = 5$) in the controls to $23.5 \pm 2.2\%$ ($N = 3$) in validamycin A-treated plants. This fraction is comprised in part of hemicellulose. We also observed a significant increase in ^{11}C partitioning into the acid-insoluble portion, from $0.3 \pm 0.03\%$ ($N = 5$) in the controls to $1.0 \pm 0.2\%$ ($N = 3$) in validamycin A-treated plants. This fraction is comprised in part of cellulose. However, the base fraction, which includes pectin and 1,3- β -glucans, showed no significant change with treatment (Table 1).

The impact on cellulose and hemicellulose biosynthesis was associated with a change in sugar metabolism. Treatment with validamycin A significantly increased the partitioning of new carbon (as ^{11}C) into fructose ($P = 0.028$) and glucose ($P = 0.044$), but decreased the partitioning into sucrose ($P = 0.046$) (Fig. 2A–C). Although the total radioactivity in the aq alcohol fraction was reduced by 20% in plants treated with validamycin A, the percentage of soluble sugars in that fraction increased by 32% ($P = 0.002$) in treated plants relative to the controls (data not shown). Furthermore, validamycin A treatment had no effect on leaf-level photo-

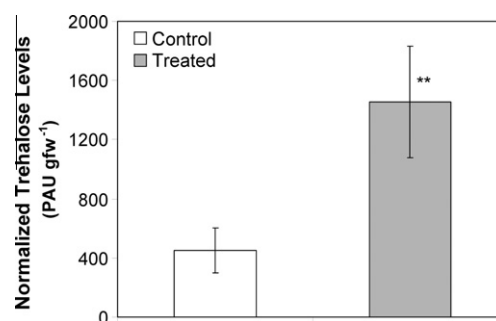


Figure 1. Effect of validamycin A after 12 h on endogenous levels of trehalose. Data presented as the integrated peak area units (PAU) normalized to gfw of leaf tissue extracted. Data show mean \pm SE ($N = 3$). Significant effects of treatment are denoted by ** ($P < 0.01$) and were detected using ANOVA single-variate analysis.

Table 1
Effect of validamycin A treatment on cell-wall [^{11}C]polysaccharides

Tissue fraction	Control	Validamycin	<i>P</i> values ^a
MeOH–H ₂ O ^b	78.5 ± 10.3	62.7 ± 5.5	0.002
NaOH ^c	10.2 ± 3.8	12.8 ± 1.0	0.805
Acetic–nitric reagent ^d	11.0 ± 1.5	23.5 ± 2.2	<0.001
Acid insoluble ^e	0.3 ± 0.03	1.0 ± 0.2	<0.001

Data show mean ± SD of % fixed ^{11}C : *N* = 5, control; *N* = 3, validamycin A.

^a *P* values were calculated using ANOVA single-variate analysis.

^b MeOH–H₂O fraction contained soluble sugars, amino acids and starch.

^c Base extract contained 1,3-β-glucans and pectins (linear 1,4-α-galacturonic acid).

^d Dilute acetic–nitric acid extract contained hemicellulose.

^e Acid indigestible portion contained cellulose.

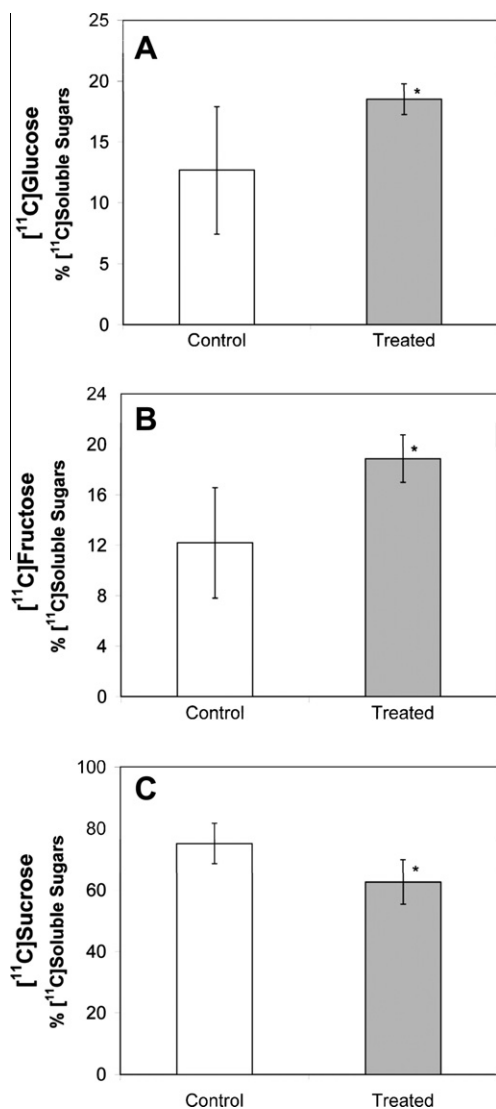


Figure 2. Effect of validamycin A after 12 h on ^{11}C -partitioning into soluble sugars: glucose (panel A), fructose (panel B) and sucrose (panel C). Data show mean ± SE (*N* = 5, control plants; *N* = 3, treatment plants). Significant effects of treatment are denoted by * (*P* < 0.05) and were detected using ANOVA single-variate analysis.

synthesis as measured by $^{11}\text{CO}_2$ fixation (Fig. 3A) and by infrared gas exchange (Fig. 3B).

Validamycin A treatment also significantly decreased the partitioning of new carbon (as ^{11}C) into phenylalanine (Fig. 4A). Furthermore, cinnamic acid levels were significantly lower (75%,

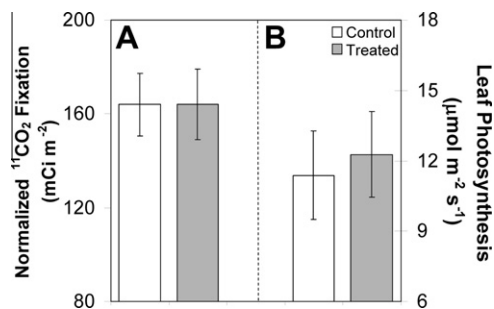


Figure 3. Effect of validamycin A treatment after 12 h on leaf-level photosynthesis: data in panel A shows $^{11}\text{CO}_2$ fixation for control and treated leaves normalized to leaf surface area exposed to the tracer; data in panel B shows net photosynthesis of the same leaves measured using infrared gas exchange. Data show mean ± SE (*N* = 3). No significant effects were noted.

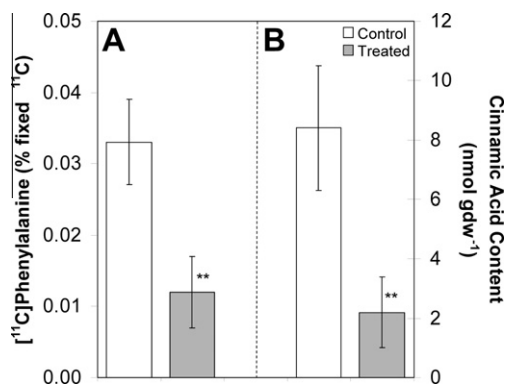


Figure 4. ^{11}C -partitioning into phenylalanine (panel A) of leaf-3 at 12 h after validamycin A treatment. Data show mean ± SE (*N* = 3). Level of cinnamic acid (panel B) at 12 h after validamycin A treatment. Data show mean ± SE (*N* = 4). Changes in endogenous cinnamic acid were used to infer changes in PAL activity. Significant effects of treatment are denoted by ** (*P* < 0.01) and were detected using ANOVA single-variate analysis.

P = 0.0045) in the validamycin A-treated plants (Fig. 4B) suggesting a decrease in PAL activity over the same time course.

We were not able to detect a change in cellulose biomass over the short 12-h timeline, but following a 4-d exposure to validamycin A changes in biomass content became evident. The cellulose levels (as % gfw averaged across leaf-2 and leaf-3) increased significantly (*P* = 0.0001) by 100% in plants treated with validamycin A (Fig. 5).

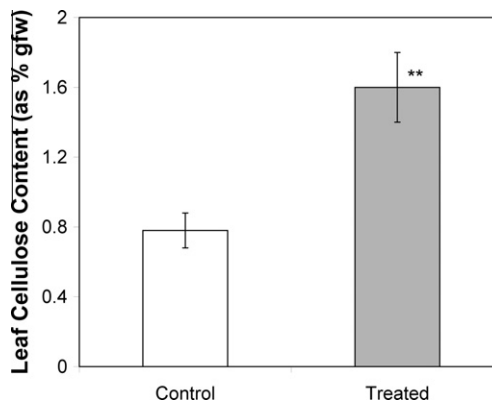


Figure 5. Effect of 4-d exposure to validamycin A on the cellulose content. Measurements were made by averaging leaf-2 and leaf-3. Data show mean ± SE (control *N* = 5 plants, treated *N* = 5 plants). Significant effects are denoted by ** (*P* < 0.01) and were detected using ANOVA single-variate analysis.

Additionally, a 4-d exposure to validamycin A treatment resulted in a 33% reduction in foliar amino acid content ($P = 0.0572$, Fig. 6A) and a more significant fourfold reduction in nitrate content ($P = 0.0003$, Fig. 6B). However, there was no effect of treatment on the soluble protein content (Fig. 6C).

Finally, validamycin A impacted foliar carbohydrate content. After 4 d of treatment leaf starch content in validamycin A-treated plants was 58% higher ($P = 0.0076$, Fig. 7A). Changes in soluble sugars matched trends seen at 12 h for new carbon partitioning (as ^{13}C) into sugars. Glucose and fructose content increased by 38% and 250%, respectively, although only the increase in fructose was significant ($P = 0.0267$, Fig. 7B and C). Sucrose content decreased significantly ($P = 0.0369$) by 60% in treated plants (Fig. 7D).

4. Discussion

Treatment of young tobacco plants with validamycin A altered the biochemical partitioning of new C and N precursors for cellu-

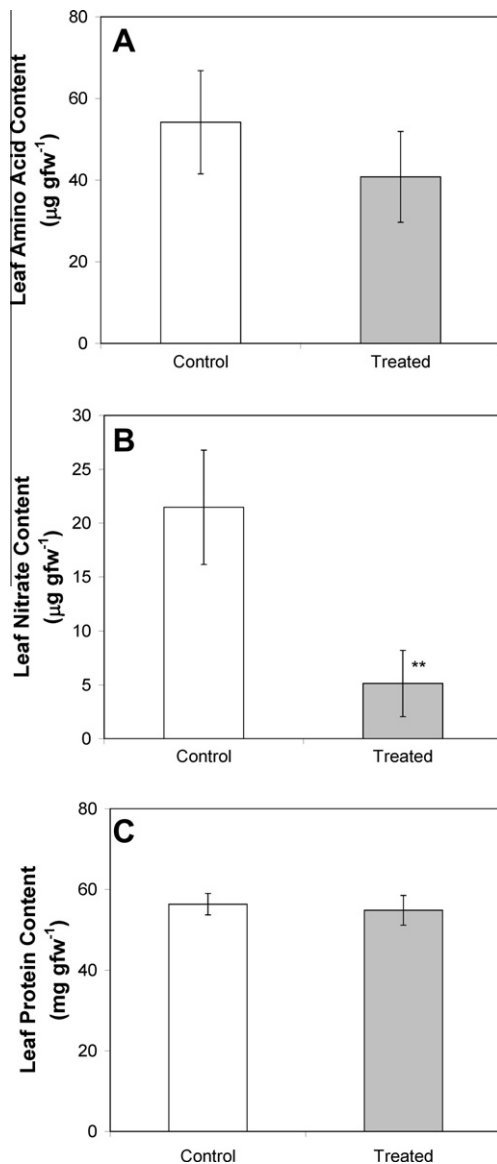


Figure 6. Effect of 4-d exposure to validamycin A on free amino acids (panel A), nitrate content (panel B) and protein content (panel C). Measurements were made on leaf-2 and leaf-3. Data show mean \pm SE ($N = 5-7$ plants). Significant effects are denoted by ** ($P < 0.01$) and were detected using ANOVA single-variate analysis.

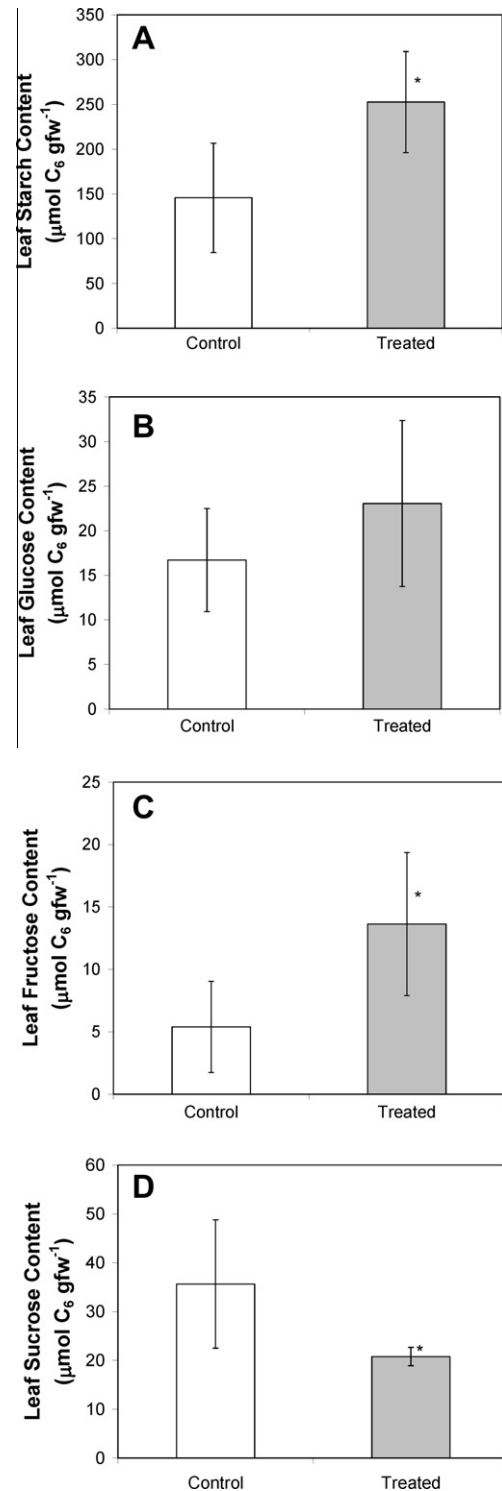


Figure 7. Effect of 4-d exposure to validamycin A on starch content (panel A), glucose content (panel B), fructose content (panel C) and sucrose content (panel D). Measurements were made on leaf-2 and leaf-3. Data show mean \pm SE ($N = 4-7$ plants). Significant effects are denoted by * ($P < 0.05$) and were detected using ANOVA single-variate analysis.

losic biomass and lignin production. This study suggests that an improved understanding of trehalose metabolism may lead to the development of bioenergy crops that provide higher quality feedstocks for the production of cellulosic biofuels.

These data support our hypothesis that inhibition of the trehalase enzyme through exogenous treatments using the antibiotic

validamycin A can have profound effects on plant carbon metabolism as seen by increased carbon partitioning into cellulosic biomass resulting from changes in central C and N metabolism. Indeed, in Arabidopsis, exogenous trehalose has been shown to induce transcripts of proteins associated with cell-wall modification,²⁷ and most particularly, a putative gene for xyloglucan fucosyltransferase that is involved in hemicellulose biosynthesis.²⁸ Furthermore, this treatment has been shown to repress transcripts of several proteins involved in amino acid biosynthesis including cystathionine γ -synthase 1, glycine hydroxymethyltransferase/serine hydroxymethyltransferase, imidazole glycerol-phosphate dehydratase, and glutamine synthetase.

Our results show a major change in carbon partitioning into soluble sugars with eventual alteration of the endogenous pools, suggesting that part of the effect of inhibiting trehalose degradation in plants may be linked to up-regulation of sucrose synthase and cell-wall invertase enzymes. Previous work demonstrated that exogenous trehalose treatment of soybean plants (*Glycine max* L. Merr.) resulted in an up-regulation of these enzymes in root tissues.²⁹ Furthermore, past studies suggest that exogenous trehalose treatment of Arabidopsis seedlings will induce expression of the gene, *ApL3*, which encodes a large subunit of ADP-glucose pyrophosphorylase resulting in increased starch accumulation in the foliar tissue.³⁰ Indeed, our results showed a similar trend with increased starch accumulation after 4 d of treatment. Consistent with an increase in sucrose metabolism and a shift to starch accumulation, our data also showed a reduction in sucrose content in plants treated with validamycin A.

The reduction in sucrose supply reduces the availability of C-skeletons for amino acid metabolism. In addition to a reduction in the size of the sucrose pool, our data also showed reduced availability of nitrate and subsequent reduction in free amino acid content suggesting that N-metabolism was also negatively impacted by the treatment. This likely resulted in the observed reduction in the amino acid phenylalanine, an important substrate for secondary metabolism, including lignin biosynthesis. We also found a decrease in the activity of PAL, the key enzyme in the first step of the phenylpropanoid pathway and cell-wall lignin biosynthesis. However, leaf protein content and photosynthesis were unaltered. The turnover of most proteins is considerably slower than the diurnal changes in leaf nitrate and free amino acids. In particular, the turnover time of rubisco, which can account for 50% of leaf nitrogen,³¹ is approximately 2 d,³² suggesting that the marked negative impact of validamycin A on nitrate and amino acid availability would likely be muted in total protein, especially considering that the reduction in available free amino acids is less than 0.05% of the mass of protein. We hypothesize that the low levels of free nitrate and amino acids are more likely to impact protein levels in developing tissues than in mature tissues. Because our experiments only targeted mature source leaves, we were not in a position to evaluate this hypothesis.

These data show that the partitioning of new carbon into cell-wall polysaccharides is finely balanced with its partitioning into cell-wall lignin. In this study, plants treated with validamycin A exhibited stunted growth patterns above ground, likely due to the lack of cell-wall lignin. Admittedly, our treatment likely elicited other unknown effects within the plant, but we would argue that the chemical inhibition approach can provide insight into the regulation of the plant's C/N resources and guidance for future molecular transformation.

In recent years, the over-expression of yeast or bacterial TPS has been reported to enhance drought tolerance in tobacco, potato, and rice crops.^{33–36} However, transgenic plants expressing a TPS1 gene from *Escherichia coli* with a constitutive promoter displayed morphological alteration, most noteworthy stunted growth similar to the response we observed in this study. However, we believe this

drawback may be overcome through expression of both TPS and TPP genes that would avoid the accumulation of trehalose-6-phosphate. Transgenic rice plants have been obtained in this way exhibiting different stress tolerances without morphological changes.³⁷ Alternatively, expression of the *Grifola frondosa* Fr. trehalose synthase gene has been shown to enhance endogenous trehalose levels in *Nicotiana tabacum* L., endowing plants with drought and salt tolerance while not inhibiting growth.³⁸

Acknowledgements

This research was supported by the US Department of Energy's Office of Biological and Environmental Science under contract DE-AC02-98CH10886, the US Department of Energy's Pre-Service Teacher program and the Graduate Research Environmental Fellowship program and the Deutscher Akademischer Austauschdienst, Bonn.

References

- Paul, M. J.; Primavesi, L. F.; Jhurreea, D.; Zhang, Y. *Annu. Rev. Plant Biol.* **2008**, *59*, 417–441.
- Delmer, D. P.; Haigler, C. H. *Metab. Eng.* **2002**, *4*, 22–28.
- Müller, J.; Aeschbacher, R. A.; Wingler, A.; Boller, T.; Wiemken, A. *Plant Physiol.* **2001**, *125*, 1086–1093.
- Müller, J.; Boller, T.; Wiemken, A. *Plant Sci.* **1995**, *112*, 1–9.
- Müller, J.; Wiemken, A.; Aeschbacher, R. *Plant Sci.* **1999**, *147*, 37–45.
- Leyman, B.; Van Dijck, P.; Thevelein, J. M. *Trends Plant Sci.* **2001**, *6*, 510–513.
- Vogel, G.; Fiehn, O.; Bressel, L. J. R. D.; Boller, T.; Wiemken, A.; Aeschbacher, R. A.; Wingler, A. *J. Exp. Bot.* **2001**, *52*, 1817–1826.
- Ramon, M.; Rolland, F. *Trends Plant Sci.* **2007**, *12*, 185–188.
- Satoh-Nagasawa, N.; Nagasawa, N.; Malcomber, S.; Sakai, H.; Jackson, D. *Nature* **2006**, *441*, 227–230.
- Gomez, L. D.; Baud, S.; Gilday, A.; Li, Y.; Graham, I. *Plant J.* **2006**, *46*, 69–84.
- Reinders, A.; Bürckert, N.; Hohmann, S.; Thevelein, J. M.; Boller, T.; Wiemken, A.; De Virgilio, C. *Mol. Microbiol.* **1997**, *24*, 687–695.
- Thevelein, J. M.; Hohmann, S. *Trends Biochem. Sci.* **1995**, *20*, 3–10.
- Blázquez, M. A.; Lagunas, R.; Gancedo, C.; Gancedo, J. M. *FEBS Lett.* **1993**, *329*, 51–54.
- Avonce, N.; Leyman, B.; Thevelein, J.; Iturriaga, G. *Biochem. Soc. Trans.* **2005**, *33*, 276–279.
- Goddijn, O. J. M.; Verwoerd, T. C.; Voogd, E.; Krutwagen, R. W. H. H.; de Graaf, P. T. H. M. *Plant Physiol.* **1997**, *113*, 181–190.
- Ferrieri, R. A.; Gray, D. W.; Babst, B. A.; Schueller, M. J.; Schlyer, D. J.; Thorpe, M. R.; Orians, C. M.; Lerda, M. *Plant Cell Environ.* **2005**, *25*, 591–602.
- Heiniger, U.; Delmer, D. P. *Plant Physiol.* **1977**, *59*, 719–723.
- Maltby, D.; Carpita, N. C.; Montezinos, D.; Kulow, C.; Delmer, D. P. *Plant Physiol.* **1979**, *63*, 1158–1164.
- Dugger, W. M.; Palmer, R. L. *Plant Physiol.* **1980**, *65*, 266–273.
- Zhong, H.; Läuchli, A. *Plant Physiol.* **1988**, *88*, 511–514.
- Dubois, M.; Gilles, K. A.; Hamilton, J. K.; Roberts, P. A.; Smith, F. *Anal. Chem.* **1956**, *28*, 350–356.
- Hanik, N.; Gómez, S.; Schueller, M.; Orians, C. M.; Ferrieri, R. A. *J. Chem. Ecol.* **2010**, *36*, 1058–1067.
- Budi-Muljono, R. A.; Looman, A. M. G.; Verpoorte, R.; Scheffer, J. J. C. *Phytochem. Anal.* **1998**, *9*, 35–38.
- Rogers, A.; Allen, D. J.; Davey, P. A.; Morgan, P. B.; Ainsworth, E. A.; Bernacchi, C. J.; Cornic, G.; Dermody, O.; Dohleman, F. G.; Delucia, E. H.; Ort, D. R.; Long, S. P. *Plant Cell Environ.* **2004**, *27*, 449–458.
- Ainsworth, E. A.; Rogers, A.; Leakey, A. D. B.; Heady, L. E.; Gibon, Y.; Stitt, M.; Schurr, U. *J. Exp. Bot.* **2007**, *58*, 579–591.
- Gibson, R. P.; Gloster, T. M.; Roberts, S.; Warren, A. J.; de Gracia, I. S.; Garcia, A.; Chiara, J. L.; Davies, G. J. *Angew. Chem., Int. Ed.* **2007**, *46*, 4115–4119.
- Bae, H.; Herman, E.; Bailey, B.; Bae, H.-J.; Sicher, R. *Physiol. Plant.* **2005**, *125*, 114–126.
- Faik, A.; Bar-Peled, M.; Derocher, A. E.; Zeng, W.; Perrin, R. M.; Wilkerson, C.; Raikhel, N. V.; Keegstra, K. *J. Biol. Chem.* **2000**, *275*, 15082–15089.
- Müller, J.; Boller, T.; Wiemken, A. *J. Plant Physiol.* **1998**, *153*, 255–257.
- Wingler, A.; Fritzius, T.; Wiemken, A.; Boller, T.; Aeschbacher, R. A. *Plant Physiol.* **2000**, *124*, 105–114.
- Spreitzer, R. J.; Salvucci Rubisco, M. E. *Annu. Rev. Plant Biol.* **2002**, *53*, 449–475.
- Piques, M.; Schulze, W. X.; Hohne, M.; Usadel, B.; Gibon, Y.; Rohwer, J.; Stitt, M. *Mol. Syst. Biol.* **2009**, *5*, 314–331.
- Holmström, K. O.; Mäntylä, E.; Welin, B.; Mandal, A.; Palvia, E. T. *Nature* **1996**, *379*, 683–684.
- Pilon-Smits, E. A. H.; Terry, N.; Sears, T.; Kim, H.; Zayed, A.; Hwang, S.; van Dun, K.; Voogd, E.; Verwoerd, T. C.; Krutwagen, R. W. H. H.; Goddijn, O. J. M. *J. Plant Physiol.* **1998**, *152*, 525–532.
- Yeo, E. T.; Kwon, H. B.; Han, S. E.; Lee, J. T.; Ryu, J. C.; Byun, M. O. *Mol. Cell* **2000**, *10*, 263–268.

36. Garg, A. K.; Kim, J. K.; Owens, T. G.; Ranwala, A. P.; Choi, Y. D.; Kochian, L. V.; Wu, R. *Proc. Natl. Acad. Sci. U.S.A.* **2002**, *99*, 15898–15903.
37. Jang, I.-C.; Oh, S.-J.; Seo, J.-S.; Choi, W.-B.; Song, S. I.; Kim, C. H.; Kim, Y. S.; Seo, H.-S.; Choi, Y. D.; Nahm, B. H.; Kim, J.-K. *Plant Physiol.* **2003**, *131*, 516–524.
38. Zhang, S.-Z.; Yang, B.-P.; Feng, C.-L.; Tang, H.-L. *J. Integr. Plant Biol.* **2005**, *47*, 579–587.